JOURNAL OF ENGINEERING SCIENCES

Volume 8, Issue 1 (2021)

Eze P. C., Ugoh C. A., Inaibo D. S. (2021). Positioning control of DC servomotor-based antenna using PID tuned compensator. Journal of Engineering Sciences, Vol. 8(1), pp. E9–E16, doi: 10.21272/jes.2021.8(1).e2

Positioning Control of DC Servomotor-Based Antenna Using PID Tuned Compensator

Eze P. C.[1*], Ugoh C. A.[2], Inaibo D. S.[2]

[1] Department of Electrical and Electronic Engineering, Covenant Polytechnic, Aba, Nigeria;
[2] Department of Power Plant and Utilities Gas Turbine Unit, NNPC WRPC, Ekpan, Warri, Nigeria

Article info:
Received: December 14, 2020
The final version received: April 26, 2021
Accepted for publication: May 1, 2021

***Corresponding email:**
paulinuseze1@gmail.com

Abstract. Direct current (DC) servomotor-based parabolic antenna is automatically positioned using control technique to track satellite by maintaining the desired line of sight for quality transmission and reception of electromagnetic wave signals in telecommunication and broadcast applications. With several techniques proposed in the literature for parabolic antenna position control, there is still a need to improve the tracking error and robustness of the control system in the presence of disturbance. This paper has presented positioning control of DC servomotor-based antenna using proportional-integral-derivative (PID) tuned compensator (TC). The compensator was designed using the control and estimation tool manager (CETM) of MATLAB based on the PID tuning design method using robust response time tuning technique with interactive (adjustable performance and robustness) design mode at a bandwidth of 40.3 rad/s. The compensator was added to the position control loop of the DC servomotor–based satellite antenna system. Simulations were carried out in a MATLAB environment for four separate cases by applying unit forced input to examine the various step responses. In the first and second cases, simulations were conducted without the compensator (PID TC) in the control loop assuming zero input disturbance and unit input disturbance. The results obtained in terms of time-domain response parameters showed that with the introduction of unit disturbance, the rise time improved by 36 % (0.525–0.336 s) while the peak time, peak percentage overshoot, and settling time deteriorate by 16.3 % (1.29–1.50 s), 43.5 % (34.7–49.8 %), and 7.6 % (4.35–4.68 s), respectively. With the introduction of the PIDTC for the third case, there was an improvement in the system's overall transient response performance parameters. Thus to provide further information on the improved performance offered by the compensator, the analysis was done in percentage improvement. Considering the compensated system assuming zero disturbance, the time-domain response performance parameters of the system improved by 94.1, 94.7, 73.1, and 97.1 % in terms of rising time (525–30.8 ms), peak time (1,290–67.9 ms), peak percentage overshoot (34.7–9.35 %), and settling time (4.35–0.124 s), respectively. In the fourth case, the compensator's ability to provide robust performance in the presence of disturbance was examined by comparing the step response performance parameters of the uncompensated system with unit input disturbance to the step response performance parameters of the compensated system tagged: with PID TC + unit disturbance. The result shows that PID TC provided improved time-domain transient response performance of the disturbance handling of the system by 91.0, 95.4, 80.0, and 93.1 % in terms of rising time (336–30.5 ms), peak time (1500–69.1 ms), peak percentage overshoot (34.7–10.0), and settling time (4.68–0.325 s), respectively. The designed compensator provided improved robust and tracking performance while meeting the specified time-domain performance parameters in the presence of disturbance.

Keywords: antenna, compensator, direct current servomotor, proportional-integral-derivative tuned compensator, positioning control.

1 Introduction

Parabolic antennas are mechanical structures that serve as essential telecommunication and broadcast equipment components used to transmit and receive signals. These antennas are used to establish communication between observers on the earth and satellite in space. Usually mounted at earth stations, parabolic antennas are employed in satellite tracking applications and are subject to environmental actions such as wind disturbance.

One of the environmental disturbance effects is the changes it can cause on the azimuth positioning control of a satellite dish. Thus, this problem has attracted

research attention in the positioning control of antennas [1]. The interests elicited by azimuth positioning control can be attributed to the significant roles and enhance performances that it would provide for efficient satellite dish communication. With many control methods proposed to achieve optimum azimuth position, such positioning remains a control problem [2].

Direct current (DC) servomotor-based control techniques have been used to position parabolic antenna for satellite tracking automatically. The application of fuzzy proportional-integral-derivative (Fuzzy-PID) control technique and conventional PID controller to achieve optimum satellite tracking performance has been proposed by Hoi et al. [3]. The step response of the Fuzzy-PID and conventional PID revealed the presence of chattering. A discrete control system using a PID control algorithm to get enhanced control of satellite dish angle was proposed by Xuan et al. [4]. The weakness of this work can be attributed to the lack of proper tuning of the PID gains for accurate results. Considering the case of overseas satellite telecommunication, Soltani et al. [5] applied a control system to direct onboard motorized antenna towards a selected satellite using Fault Tolerant Control (FTC) technique. However, the FTC scheme was not sufficiently robust to address the detected fault in the response. The uses of PID and Linear Quadratic Gaussian (LQG) or Linear Quadratic Regulator (LQR) for positioning control of antenna azimuth were presented by [6, 7]. The performance of either PID-LQG or PID-LQR degrades due to nonlinearity and delay as the system approaches the setpoint. Although a much-improved performance in terms of reduced settling time and reduced overshoot was reported by Okumus et al. [8] to have been achieved using Fuzzy Logic Controller (FLC) and Self-Tuning Fuzzy Logic Controllers (STFLC), the chattering process was said to be the weakness of the system. Uthman and Sudin [2] used the PID controller and state feedback controller technique for the control of satellite antenna azimuth position control. However, the system is prone to a nonlinear effect. Fandak and Okumus [9] applied PID, FLC, and Sliding Model Control (SMC) techniques for antenna azimuth position control. It was reported that the performances of the PID and FLC controllers were affected by periodic noise, while the SMC controller was not affected. However, the weaknesses of SMC control is the chattering effect. In order to improve the performance of the antenna position control system, Onyeka et al. [10] used a Model Predictive Controller (MPC). Though the design specifications were realized in work, the designed MPC parameter seems inadequate to offer robust performance in the presence of disturbance. Application of PID controller and a low pass filter applied to setpoint input aim at improving the performance response of mobile satellite antenna network within Nigeria was presented by Eze et al. [11]. Though the system was reported to have achieved better response performance than the existing system, there was weakness in providing optimum performance in terms of rising time and peak time compared to the existing system, and the effect of disturbance was not considered. Because of these proposed systems and the nonlinear characteristics of the satellite antenna due to the uncertainties caused by wind actions and other environmental disturbances, there is still a control problem. There is a need for improved robustness to disturbance handling while maintaining reduced tracking error for effective antenna azimuth position control, which justifies this study.

In this paper, the objective is to design a compensator to address the problem of antenna azimuth position control deterioration caused by disturbance for quality communication and achieving the design requirements standard of a practical industrial system in the time domain given as the rising time of less than or equal to 4 s, peak percentage overshoot of less than or equal to 10 % and settling time of less than or equal to 5 s [7]. A controller is proposed to ensure robust performance for effective satellite tracking and line of sight operation even in the presence of disturbance. The remaining part of this paper is divided into four sections, namely, system description and DC servomotor modeling, design of PID TC, simulation results and discussion, and conclusion.

2 Research Methodology

2.1 System description

The structure of a DC servomotor-based antenna positioning control system is presented in the form of a block diagram in Figure 1.

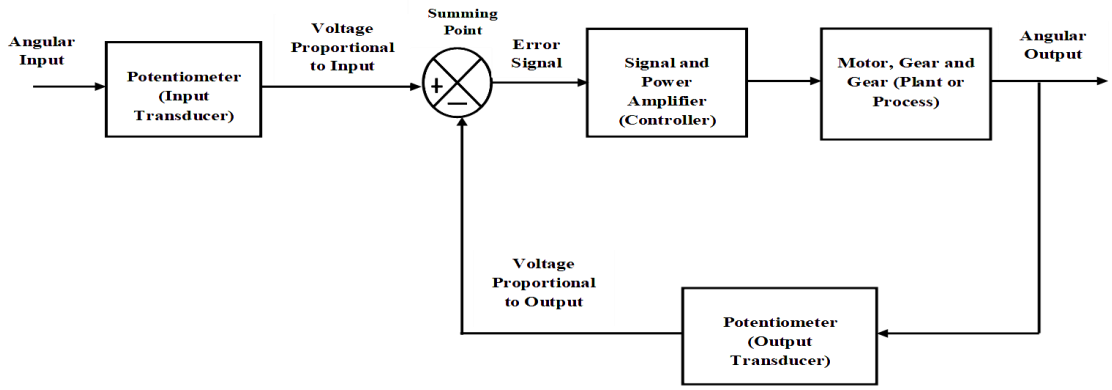

Figure 1 – Block diagram of position control satellite antenna

The system has two transducers, which are potentiometers for converting angular input and angular output (mechanical quantities) to equivalent voltage values (electrical quantities) at the input and output. The angular input is the reference position, which is the first input to the summing point after being converter to equivalent voltage magnitude (voltage proportional to input) by the input potentiometer and serves as the azimuth's desired position or elevation motor is required to attain. The second input to the summing point is the voltage proportional to the output obtained from the angular output (output position) conversion by the feedback potentiometer. The difference between the two inputs to the summing point is the error signal fed into the controller that manipulates the error signal and gives out an appropriate manipulated or control signal to rotate the motor in either direction in line with the sign of the error signal, positive or negative [7]. The error signal reduces to zero as the desired position is approached, thereby bringing the motor to a stop [7].

2.2 DC servomotor modeling

It is necessary to provide the mathematical expression of the dynamics of the DC motor, which is very important in realizing the paper's objective. Figure 2 is an illustration of an armature-controlled DC motor for the antenna positioning control system.

The DC motor diagram in Figure 2 consists of two main parts: the electrical components (part A) and the mechanical components (part B). The applied voltage to the motor's armature varies without changing the applied voltage to the field in armature controlled separately excited DC motor. Applying Kirchhoff's voltage law (KVL) and the law of dynamic motion to the DC motor in Figure 2 gives the following mathematical expressions:

$$V_a(t) = R_a I_a(t) + L_a \frac{dI_a(t)}{dt} + E_b(t); \quad (1)$$

$$E_b(t) = K_B \omega_m(t) = K_B \frac{d\theta(t)}{dt}; \quad (2)$$

$$T_m(t) = K_T I_a(t), \quad (3)$$

where $V_a(t)$ – applied voltage; $E_B(t)$ – back electromotive force (emf); $T_m(t)$ – motor torque; R_a – armature resistance; $I_a(t)$ – armature current; L_a – armature inductance; K_B – back-emf constant; K_T – motor torque constant, $\omega_m(t)$ – the angular velocity; $\theta(t)$ – the angular position.

Substituting equation (2) into (1) gives

$$V_a(t) = L_a \frac{dI_a(t)}{dt} + R_{aI_a}(t) + K_B \frac{d\theta(t)}{dt}. \quad (4)$$

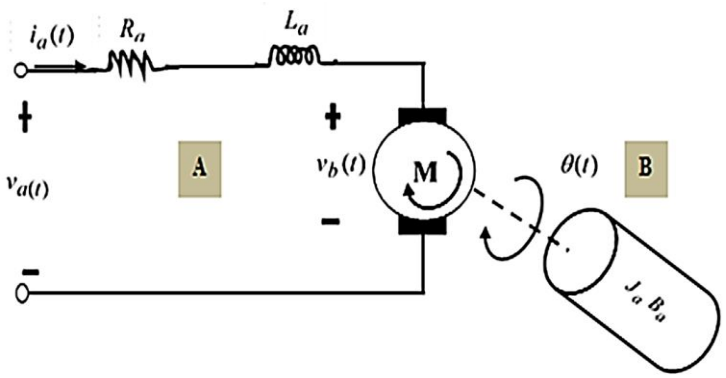

Figure 2 – DC motor diagram

The equation of the torque is given by:

$$J_a \frac{d^2\theta(t)}{dt} + B_a \frac{d\theta(t)}{dt} = K_T I_a(t). \quad (5)$$

Taking the Laplace transform of equations (4) and (5) assuming zero initial conditions give:

$$V_a(s) = L_a s I_a(s) + R_a I_a(s) + K_B s\theta(s) \quad (6)$$

$$J_a s^2\theta(s) + B_a\theta(s) = K_T I_a(s) \quad (7)$$

Making current the subject in (6) and (7), and equating both gives:

$$\frac{V_a(s) - K_B s\theta(s)}{R_a + L_a s} = \frac{J_a s^2\theta(s) + B_a s\theta(s)}{K_T}. \quad (8)$$

The ratio of the output (angular output) to the applied voltage is given by:

$$\frac{\theta(s)}{V_a(s)} = \frac{K_T}{s[(R_a + L_a s)(J_a s + B_a) + K_T K_B]}. \quad (9)$$

The block model of the DC servomotor dynamic is shown in Figure 3.

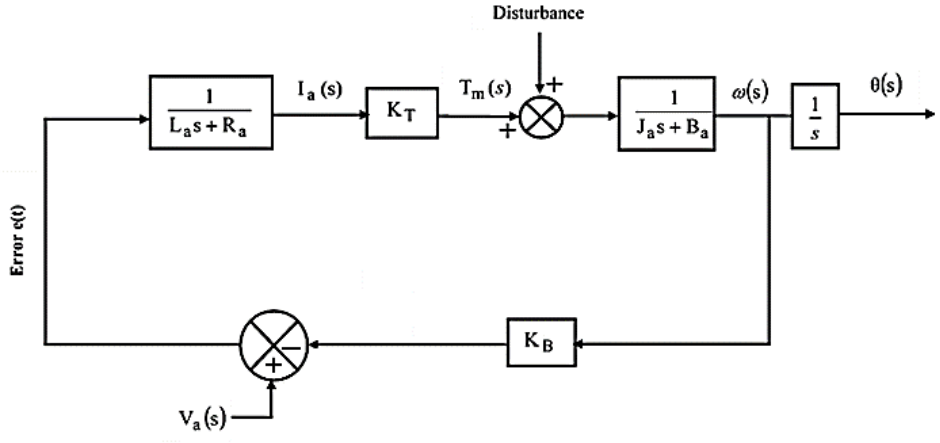

Figure 3 – Closed-loop block model of DC motor dynamic

The transfer function from reference input (applied voltage) to the angular velocity as shown in Figure 3 (assuming disturbance is zero) is given by:

$$\frac{\omega(s)}{V_a(s)} = \frac{K_T}{\left[(R_a + L_a s)(J_a s + B_a) + K_T K_B\right]}. \quad (10)$$

The transfer function expressions in equations (9) and (10) are relevant to the electrical-mechanical motion analysis of the DC motor responsible for the antenna's azimuth/elevation positioning.

The armature circuit inductance L_a is usually negligible in a fixed motor [13] and $K_T = K_a$, $R_a >> L_a$ [7]. Thus, equation (10) is reduced to:

$$\frac{\theta(s)}{V_a(s)} = \frac{K_T/R_a}{J_a s^2 + s\left(B_a + K_T K_B/R_a\right)}. \quad (11)$$

Substituting the equivalent values for the moment of inertia and the viscous friction coefficient, equation (11) is expressed:

$$\frac{\theta(s)}{V_a(s)} = \frac{K_T/R_a J_m}{J_m s^2 + s\left(B_m + K_T K_B/R_a\right)}. \quad (12)$$

Dividing numerator and denominator by J_m, equation (12) is expressed given by:

$$\frac{\theta(s)}{V_a(s)} = \frac{K_m}{s(s + a_m)}. \quad (13)$$

where B_m – the equivalent viscous friction coefficient; J_m – the equivalent moment of inertia; K_m – motor and load gain; a_m – the motor and load pole:

$$K_m = \frac{K_T}{R_a J_m},\ a_m = \frac{B_m R_a + K_T K_B}{J_m R_a}.$$

The parameters of the system, as well as the DC servomotor, are given in Table 1. Using a gear ratio, the transfer function relating the angular position and armature voltage is given by:

$$\frac{\theta(s)}{V_a(s)} = 0.1 \times \frac{K_m}{s(s + a_m)} = \frac{0.2083}{s(s + 1.71)} \quad (14)$$

With a = 100, K_1 = 100, and K_{pot} = 0.318 defined in Table 1, the closed-loop diagram shown in Figure 4 has a transfer function for antenna DC servomotor system given by:

$$G_p(s) = \frac{\theta_o(s)}{\theta_i(s)} = \frac{6.63K}{s^3 + 101.71s^2 + 171s + 6.63K}. \quad (15)$$

According to the Routh-Hurwitz criterion, the system will give a stable response with a gain K of the preamplifier in the range $0 < K < 2{,}623$ [1, 7, 12]. The gain has been chosen in this paper to be 100 for design convenience and energy consumption reduction.

Table 1 – Parameters of the model with DC servomotor [1, 4, 7]

Quantity	Definition	Value
a	Power amplifier pole	100
a_m	Motor and load pole	1.71
b_a	Motor dampening constant	0.01 N·m/rad
B_L	Load dampening constant	1 N·m·s/rad
B_m	Viscous friction coefficient	0.02 N·m·s/rad
J_a	Motor inertia constant	0.02 kg·m^2
J_L	Load inertia constant	1 kg·m^2
J_m	Equivalent moment of inertia	0.03 kg·m^2
K	preamplifier gain	–
K_1	Power amplifier gain	100
K_B	Back emf constant	0.5 V·s/rad
K_g	Gear ratio	0.1
K_m	Motor and load gain	2.083
K_{pot}	Potentiometer gain	0.318
K_T	Motor torque constant	0.5 N·m/A
L_a	Motor armature inductance	0.45 H
N	Turns on potentiometer	10
$N_1/N_2/N_3$	Gear teeth, respectively	25/250/250
R_a	Motor armature resistance	8 Ohm
V	Voltage across potentiometer	10 V

The closed-loop block diagram of the antenna DC servo motor control system is shown in Figure 4.

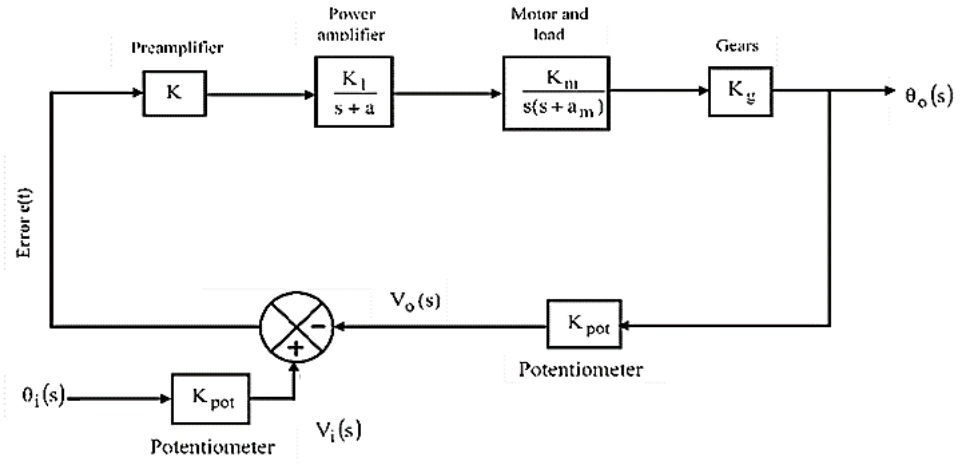

Figure 4 – Closed-loop block diagram of antenna DC servomotor control system

2.3 Design of PID tuned compensator and system configuration

The compensator is used in a control system when the response is very unstable and required to be stabilized to achieve specified performance. Since the studied DC servomotor-based satellite antenna shows some degree of instability and it is prone to environmental disturbance, a compensator has been designed using the Control and Estimation Tool Manager (CETM) of MATLAB and added to the position control loop to achieve improved transient response and robustness with better stability performance. The design method is based on PID Tuning using robust response time as the tuning method with interactive (adjustable performance and robustness) design mode in the frequency domain. The tuning bandwidth is 40.3 rad/s. The closed diagram of the system with the designed compensator and an input disturbance is shown in Figure 5.

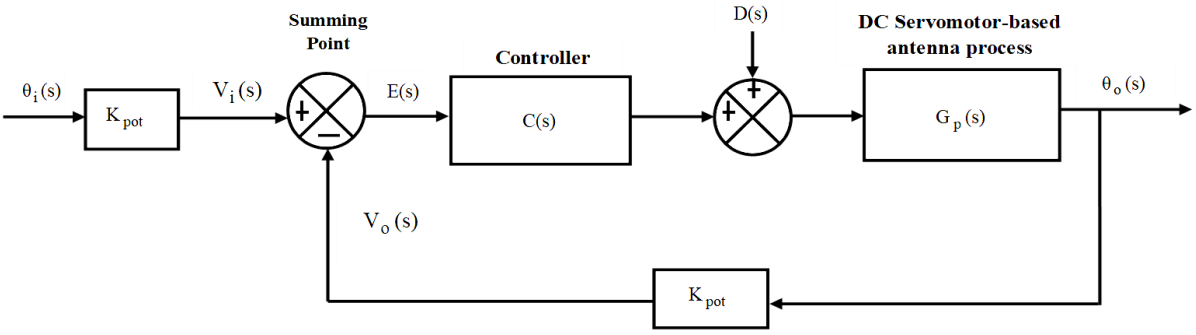

Figure 5 – Block diagram of DC servomotor-based position control

The compensator is given by:

$$C(s) = 7.2507\frac{(1+0.32s)(1+2.8s)}{s(1+0.0024s)}. \qquad (16)$$

The closed-loop transfer function without the compensator assuming unit disturbance is given by:

$$G_d = \frac{\begin{array}{c}1326s^9 + 4.046e05s^8 + 4.183e07s^7 + 1.537e09s^6 + 7.869e09s^5 + \\ 4.941e10s^4 + 1.319e11s^3 + 3.992e11s^2 + 4.984e11s + 7.729e11\end{array}}{\begin{array}{c}s^{12} + 406.8s^{11} + 6.275e04s^{10} + 4.421e06s^9 + 1.296e08s^8 + 8.809e08s^7 + 6.441e09s^6 \\ + 2.466e10s^5 + 9.742e10s^4 + 2.222e11s^3 + 5.228e11s^2 5.98e11s + 7.729e11\end{array}} \qquad (17)$$

The closed-loop transfer function with the compensator assuming zero disturbance is given by:

$$G_{cp}(s) = \frac{C(s)\times G_p(s)}{1 + C(s)\times G_p(s)}. \qquad (18)$$

Hence substituting the expressions in equations (15) and (16) into (18) gives:

$$G_{cp}(s) = \frac{1.7947e06(s+0.3571)(s+3.125)}{(s+429.3)(s+3.443)(s^2+85.28s+3989)}. \qquad (19)$$

Using a similar approach for closed-loop transfer function assuming a step input disturbance $D(s)$ in [14], the expression for the closed-loop representation of the DC servomotor-based antenna position control system in Figure 5 is given by:

$$\theta_o(s) = G_{cp}(s) + G_{dp}(s)\,; \qquad (20)$$

$$\theta_o(s) = \theta_i(s)\left[\frac{C(s)\times G_p(s)}{1+C(s)\times G_p(s)}\right] + D(s)\left[\frac{G_p(s)}{1+C(s)\times G_p(s)}\right], \qquad (21)$$

where $G_{dp}(s)$ is the expression for the transfer function due to unit disturbance $D(s)$ in equation (21), and it is given by:

$$G_{dp}(s) = \left[\frac{G_p(s)}{1+C(s)\times G_p(s)}\right]. \qquad (22)$$

Therefore,

$$G_{dp}(s) = \frac{3.6942e-4(s+416.7)(s+100.1)(s^2+1.643s+6.626)}{(s+100.1)(s+3.125)(s^2+1.643s+6.626)} \qquad (23)$$

Hence, equation (20) becomes:

$$\theta_o(s) = \frac{3.6942e-4(s+2010)(s+100.1)(s^2+0.6936s+0.1205)(s^2+6.405s+10.3)}{(s^2-1082s+2.426e06)} \qquad (24)$$
$$\frac{(s+429.3)(s+100.1)(s+3.443)(s+3.125)(s+0.3571)(s+0.3397)}{(s^2+1.643s+6.626)(s^2+85.28+3989)}$$

A detailed dynamic representation of the loop configuration of a DC servomotor-based satellite antenna position control system with unit step input applied to it represents the reference position the system is required to attain for an optimum line of sight to ensure quality communication is required achieved. When subject to environmental disturbance (using unit input), the dynamic of the system has been presented as well.

3 Results

In this section, the results and analysis of the system's performance based on simulation conducted in terms of unit step input in the MATLAB environment are presented as follows. The simulations conducted are basically for four cases and include the system without a compensator (zero disturbance), without compensator (plus unit input disturbance), with compensator (zero disturbance), and with compensator (plus unit input disturbance). The time-domain step response performance analysis of the system for each case is presented in Table 2.

Parameters t_r, t_p, *POS*, and t_s are the rise time in second, peak time in second, peak percentage overshoot, and settling time in second, respectively.

Table 2 – Time domain transient response performance parameters of the system to the unit step input

System	t_r(s)	t_p(s)	POS(%)	t_s(s)
Without a compensator (zero disturbance)	0.525	1.29	34.7	4.35
Without compensator (plus unit input disturbance)	0.336	1.50	49.8	4.68
with compensator (zero disturbance)	0.0308	0.0679	9.35	0.124
with compensator (plus unit input disturbance)	0.0305	0.0691	10	0.325

The responses of the system are presented in Figures 6–11.

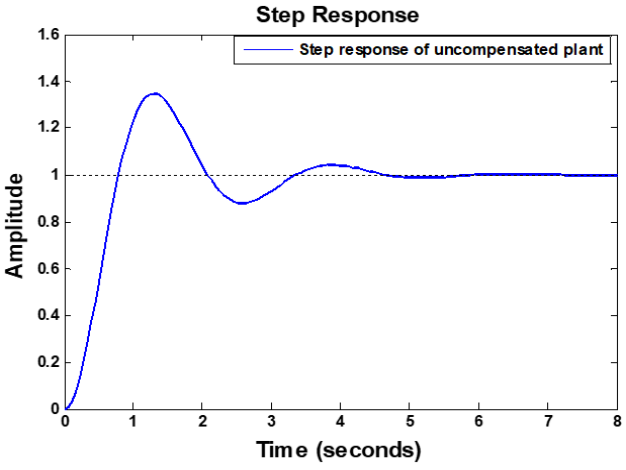

Figure 6 – Step response of the system (uncompensated)

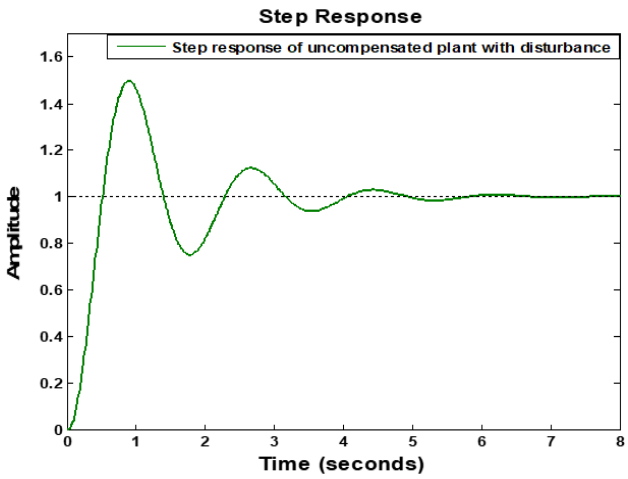

Figure 7 – Step response of the system with unit input disturbance (uncompensated)

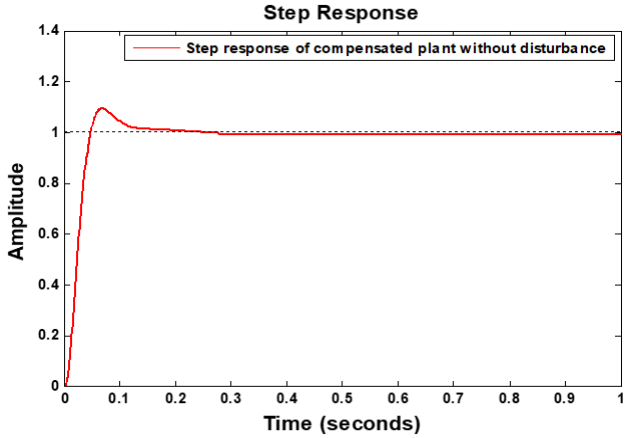

Figure 8 – Step response of the system with PID TC (zero disturbance)

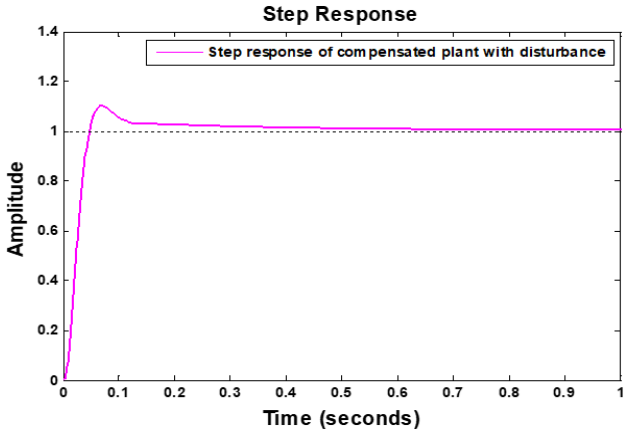

Figure 9 – Step response of the system with PID TC plus disturbance

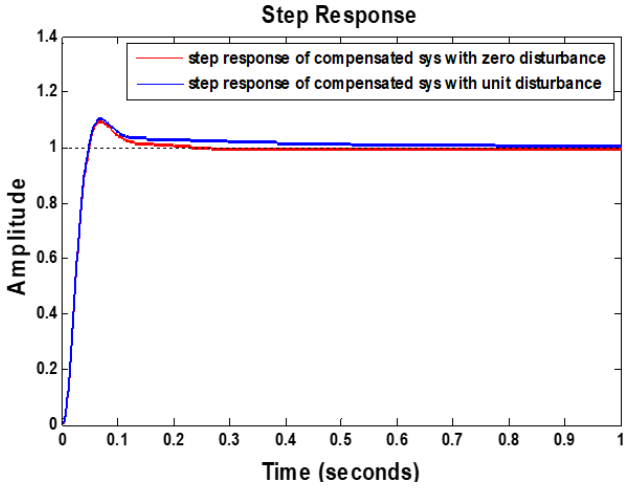

Figure 10 – Step responses of the system with PID TC (with and without disturbance)

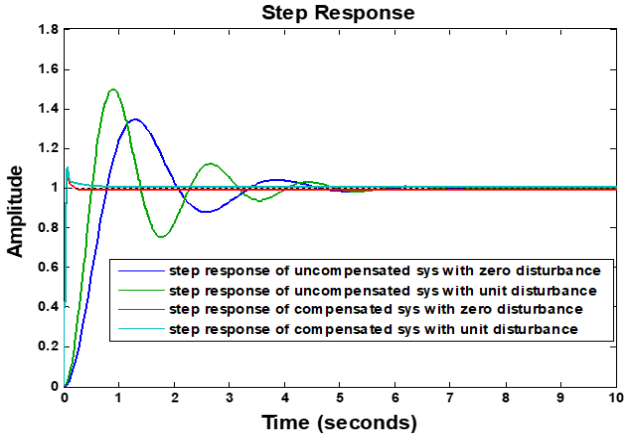

Figure 11 – Step responses of the system for uncompensated and compensated with and without disturbance

The percentage improvement in time domain performance parameters of the system with the introduction of PID TC is presented in Table 3.

The analysis was done using expression

$$\%\text{Improvemnet} = \frac{P_{\text{uncompensa ted}} - P_{\text{compensate d}}}{P_{\text{uncompensa ted}}} \times 100 \,, \quad (25)$$

where $P_{uncompensated}$, and $P_{compensated}$ are the performance of the system without and with PID TC, respectively.

4 Discussion

The time-domain step response performance characteristics of the system for each case simulated in this paper are shown in Table 1. While Table 2 shows the percentage improvement of the system based on the introduction of PID TC in terms of system with compensator and system plus disturbance with compensator. It can be deduced from Table 2 that with the uncompensated system, considering the high peak percentage overshoot, there is a considerable instability effect associated with the performance of the antenna positioning for optimum response. From the point of view of the uncompensated system, it can be seen looking at Table 2 that with the introduction of unit disturbance, the rise time improved by 36 % (0.525 s to 0.336 s) while the peak time, peak percentage overshoot, and settling time deteriorate by 16.3 % (1.29 s to 1.50 s), 43.5 % (34.7 % to 49.8 %), and 7.6 % (4.35 s to 4.68 s), respectively.

With the introduction of the PID TC, it can be seen in Table 1 that there is an improvement in the overall transient response performance of the time domain parameters of the system. Thus to provide further information on the improved performance offered by the compensator, the analysis has been done in percentage, as shown in Table 3.

Table 3 – Percentage improvement in time domain performance parameters based on PID TC introduction, %

System	Rise time	Peak time	Peak overshoot	Settling time
With PIDTC (zero disturbance)	94.1	94.7	73.1	97.1
With PIDTC + unit disturbance	91.0	95.4	80.0	93.1

Considering zero-disturbance compensated systems, it can be deduced from Table 2 that the time-domain response performance parameters of the system improved by 94.1, 94.7, 73.1, and 97.1 % in terms of rising time (0.525 s to 0.0308 s), peak time (1.29 s to 0.0679 s), peak percentage overshoot (34.7 % to 9.35 %), and settling time (4.35 s to 0.124 s), respectively.

The compensator's ability to provide robust performance in the presence of disturbance can be seen in Table 2 by comparing the step response performance parameters of the uncompensated system with unit disturbance to the step response performance parameters of the compensated system with unit disturbance, tagged: with PID TC + unit step disturbance. The result shows that PID TC provided improved time-domain transient response performance of the disturbance handling of the system by 91.0, 95.4, 80.0, and 93.1 % in terms of rising time (0.336 s to 0.0305 s), peak time (1.50 s to 0.0691 s), peak percentage overshoot (34.7 to 10.0), and settling time (4.68 s to 0.325 s).

5 Conclusions

The primary objective of this paper is to design a compensator that will provide robust response performance in the presence of disturbance so as to achieve improved error tracking and robustness. In this case, the tracking of unit step input represents the desired position for a DC servomotor-based satellite antenna position control system and corresponds to an effective line of sight operation for quality communication. With the modeling of the system and the subsequent design of PID TC, simulations were conducted basically for two categories. The first category of simulations is when the PID TC has not been added to the control loop, while the second category is when the PID TC has been added into the loop. The results obtained show that the designed compensator provided improved robust and tracking performance while meeting the specified time-domain performance parameters in the presence of disturbance.

References

1. Nise, N. S. (2011). *Control System Engineering*. 6th ed. John Wiley & Sons.
2. Uthman, A., Sudin, S. (2018). Antenna azimuth position control system using PID controller & state-feedback controller approach. *International Journal of Electrical and Computer Engineering*, Vol. 8(8), pp. 1539–1550, https://doi.org/10.11591/ijece.v8i3.pp1539-1550.
3. Hoi, T. V., Xuan, N. T., Duong, B. G. (2015). Satellite tracking control system using Fuzzy PID controller. *VNU Journal of Science: Mathematics and Physics*, Vol. 31(1), pp. 36–46.
4. Xuan, L., Estrada, J., Di Giacomandrea, J. (2009). *Antenna Azimuth Position Control System Analysis and Implementation*. Design Problem.
5. Soltani, M. N., Zamanabadi, R., Wisniewski, R. (2010). Reliable control of ship-mounted satellite tracking antenna. *IEEE Transactions on Control Systems Technology*, Vol. 19(1), pp. 221–228, https://doi.org/10.1109/TCST.2010.2040281.
6. Ahmed, M., Mohd Noor, S. B., Hassan, M. K., he Soh, A. B. (2014). A Review of strategies for parabolic antenna control. *Australian Journal of Basic and Applied Sciences*, Vol. 8(7), pp. 135–148.
7. Aloo, L. A., Kihato, P. K., Kamau, S. (2016). DC servomotor-based antenna positioning control system design using hybrid PID-LQR controller. *European International Journal of Science and Technology*, Vol. 5(2), pp. 17–31.
8. Okumus, H. I., Sahin, E., Akyazi, O. (2013). Antenna azimuth position control with fuzzy logic and self-tuning fuzzy logic controllers. *IEEE International Conference on Electrical and Electronics Engineering (ELECO)*, pp. 477–481.
9. Fandakl, S. A., Okumus, H. I., (2016). Antenna azimuth position control with PID, fuzzy logic and sliding mode controller. *2016 International Symposium on Innovations in Intelligent Systems and Applications (INISTA)*, pp. 1–5, https://doi.org/ 10.1109/INISTA.2016.7571821.
10. Onyeka, E. B., Chidiebere, M., Nkiruka, A. P. (2018). Performance improvement of antenna positioning control system using model predictive controller. European *Journal of Advances in Engineering and Technology*, Vol. 5(9), pp. 722–729.
11. Eze, P. C., Jonathan, A. E., Agwah, B. C., Okoronkwo, E. A. (2020). Improving the performance response of mobile satellite dish antenna network within Nigeria. *Journal of Electrical, Electronics, Control and Computer Science*, Vol. 6(21), pp. 25–30.
12. Ogata, K. (2010). *Modern Control Engineering*. 5th ed. Prentice-Hall Inc. USA, pp. 95–96.
13. Mbaocha, C., Eze, P., Uchegbu, V. (2015). Positioning control of drilling tool device for high speed performance. *International Journal of Electrical and Electronics Research*, Vol. 3(2), pp. 138–145.
14. Eze, P. C., Onuora, A. E., Ekengwu, B. O., Muoghalu, C., Aigbodioh, F. A. (2017). Design of a robust PID controller for improved transient response performance of a linearized engine idle speed model. *American Journal of Engineering Research*, Vol. 6(8), pp. 305–513.